RESEARCH

Check for
updates

Metabolomic profiling of exosomes reveals age-related changes in ovarian follicular fluid

Yanqiong Gu[1†], Xunyi Zhang[2†], Ruixue Wang[1], Yingying Wei[1], Hao Peng[1], Kai Wang[1], Han Li[1*] and Yazhong Ji[2*]

Abstract

Background Female fertility declines with increased maternal age, and this decline is even more rapid after the age of 35 years. Follicular fluid (FF) is a crucial microenvironment that plays a significant role in the development of oocytes, permits intercellular communication, and provides the oocytes with nutrition. Exosomes have emerged as being important cell communication mediators that are linked to age-related physiological and pathological conditions. However, the metabolomic profiling of FF derived exosomes from advanced age females are still lacking.

Methods The individuals who were involved in this study were separated into two different groups: young age with a normal ovarian reserve and advanced age. The samples were analysed by using gas chromatography–time of flight mass spectrometry (GC–TOFMS) analysis. The altered metabolites were analysed by using Kyoto Encyclopedia of Genes and Genomes (KEGG) analysis to identify the functions and pathways that were involved.

Results Our data showed that metabolites in exosomes from FF were different between women of young age and women of advanced age. The set of 17 FF exosomal metabolites ($P \leq 0.05$) may be biomarkers to differentiate between the two groups. Most of these differentially expressed metabolites in FF were closely involved in the regulation of oocyte number and hormone levels.

Conclusions In this study, we identified differences in the metabolites of exosomes from FF between women of young age and women of advanced age. These different metabolites were tightly related to oocyte count and hormone levels. Importantly, these findings elucidate the metabolites of the FF exosomes and provide a better understanding of the nutritional profiles of the follicles with age.

Keywords Follicular fluid, Exosome, Metabolomics, Advanced age, Ovary

†Yanqiong Gu and Xunyi Zhang have contributed equally to this work.

*Correspondence:
Han Li
lihan_shtj@163.com
Yazhong Ji
jiyazhong@hotmail.com
[1] Clinical and Translational Research Center, Shanghai Key Laboratory of Maternal-Fetal Medicine, Shanghai Institute of Maternal-Fetal Medicine and Gynecologic Oncology, Shanghai First Maternity and Infant Hospital, School of Medicine, Tongji University, Shanghai, No. 2699, West Gaoke Road, Shanghai 201204, China
[2] Reproductive Medicine Center, Tongji Hospital Affiliated to Tongji University, Shanghai, , No. 389 Xincun Road, Shanghai 200065, China

Background

Female fertility declines with increased maternal age, and it particularly declines more rapidly after the age of 35 years, with a more considerable decline being observed at an age of 45–50 years when menopause normally occurs [1, 2]. Compared with women who get pregnant at a young age, women over the age of 35 years have a higher risk of pregnancy complications [3, 4]. Previous studies have suggested that the age-related decline in female fertility may be related to a decrease in oocyte quality and granulosa cell dysfunction [5, 6]. However, the process of ovarian aging remains largely unexplored. Follicular fluid (FF) is composed of both the transfer fluid of blood plasma constituents that cross the blood

follicular barrier and of the secretory active substance of granulosa and theca cells [7, 8]. It contains hormones, proteins, amino acids, enzymes, fatty acids, cytokines, anticoagulant factors, and antiapoptotic factors [7, 9]. Moreover, FF provides an important microenvironment and nutrition for oocyte development and permits intercellular communication and maturity inside of the follicle [10–12]. The FF composition reflects changes in granular layer secretion and the inner membrane, as well as changes in plasma composition caused by physiological or pathological processes [13].

Extracellular vesicles (EVs) have emerged as being important mediators for communication between cells and organs. EVs are classified into exosomes, microvesicles, and apoptotic bodies (according to their different size, biogenesis, and function) [14]. Exosomes are nano-sized membrane vesicles (30–150 nm in diameter) [15] that contain a variety of signalling molecules, such as mRNAs, microRNAs, proteins, and metabolites [16]. The transfer of these components among different cells can have an impact on biological activities [16, 17]. Exosomes have been linked to age-related pathological conditions and a dysfunctional mitochondrial–lysosomal axis [18]. Additionally, senescent cell-derived EVs may act as pro-gerontic factors [19, 20]. Increasing evidence indicates that EVs play important roles in the aging process [21]. Importantly, in exosome formation, cytosolic small molecules (metabolites), including sugars, amino acids, nucleotides, different enzymatic cofactors, and redox regulatory molecules, are also involved in these small vesicles [22–24]. EVs can act as independent metabolic units, with potential effects on the physiology of their microenvironment [25]. Metabolomics may be a powerful tool for discovering the underlying biological processes of aging [26].

Exosomes can be isolated from follicular, uterine, and oviductal fluids [27–30]. Recent studies have suggested that exosomes in FF may carry miRNAs for steroidogenesis and follicular development [17, 31, 32]. Through a comprehensive analysis of the composition of FF exosomes, there exists a promising opportunity to identify specific biomarkers and additional information about the ovarian state. However, as part of the exosome cargo, metabolites have not received enough attention thus far. In this study, we aimed to identify differences in the metabolites of exosomes from FF between women of young age and women of advanced age.

Materials and methods
Characteristics of patients
All of the females underwent in vitro fertilization (IVF) or intracytoplasmic sperm injection (ICSI) at Shanghai First Maternity and Infant Hospital from February 2022 to December 2022. Women with medical disorders (such as polycystic ovary syndrome [PCOS], endometriosis, cancer, or a history of ovarian surgery), that could affect follicular development were excluded from the study. Participants were divided into two groups: a young control group (age < 35, $n = 30$) and an advanced age group (age ≥ 40, $n = 30$).

This study was approved by the Scientific and Ethical Committee of the Shanghai First Maternity and Infant Hospital affiliated with Tongji University. All of the participants gave their written informed consent and the collection of samples was approved.

Exosome isolation
All of the patients received controlled ovarian hyperstimulation by using a combination of gonadotropin-releasing hormone (GnRH) agonist or antagonist and recombinant follicle-stimulating hormone (FSH). FF was collected by using transvaginal ultrasound-guided aspiration from dominant follicles (> 18 mm), (yielding 2–3 ml) at 34 to 36 h after the administration of 10,000 IU human chorionic gonadotropin (hCG). The supernatants were stored at − 80 ℃ after centrifugation at 3000×g for 15 min to remove cell debris and other particles. The FF exosomes were collected with an ExoQuick-TC Exosome Precipitation Solution Kit (System Biosciences, Palo Alto, CA), which is widely used to obtain exosomes from different body fluids. However, the obtained exosome sample was not homogenous. In brief, 250 μl of ExoQuick Solution was added to 1 ml of FF in a 1:4 ratio. The mixture was thoroughly mixed and left to incubated overnight at a temperature of 4 ℃. After incubation, the mixture was centrifuged at 1500×g for 30 min at 4 ℃ and the supernatant was carefully removed. The resulting exosome pellet was then resuspended in 500 μl of PBS and passed through a 0.22 μm filter to obtain the desired solution.

Transmission electron microscopy
Exosomes were analysed via transmission electron microscopy (TEM) as previously described [33, 34]. Twenty microlitres of exosome suspension (5 μg/μl) was fixed on a continuous grid, after which it was negatively stained with 2% uranyl acetate solution for 1 min and air-dried. The samples were then observed by using an FEI Tecnai G2 spirit transmission electron microscope (FEITM, Hillsboro, OR) at an acceleration voltage of 120 kV [35].

Nanoparticle tracking analysis
Nanoparticle tracking analysis (NTA) measurements were performed by using a NanoSight NS300 instrument (Malvern Panalytical, Malvern, UK) with a 488-nm laser and sCMOS camera module (Malvern Panalytical). Flow

measurements were performed at a flow rate of 50. Three 60-s measurements were taken and the captured data were analysed by using NTA 3.2 software [35].

Western blot

The concentration of proteins was quantified by using the Pierce BCA Protein Assay Kit (Thermo Fisher Scientific, Waltham, MA) following the manufacturer's instructions. Proteins were separated via gel electrophoresis on 10% SDS-PAGE gels and then transferred to PVDF membranes via electroblotting [17]. After blocking with 5% BSA, the blots were probed with exosome-specific antibodies (CD9, CD63, CD81, and Hsp70; System Biosciences) at 4 ℃ overnight. After washing the membranes, they were incubated with secondary antibodies, and proteins were visualized by using enhanced chemiluminescence reagents (Thermo Fisher Scientific) [17].

Metabolomics analyses

Two internal standards were added to exosomes from 1 ml of FF in each serum sample. Gas chromatography–time of flight mass spectrometry (GC–TOFMS) was used to analyse the samples in the order of "control and aging" by using the electron ionization mode (utilized instrument used: Pegasus HT, Leco Corp., St. Joseph, MI). One quality control (QC) sample and one blank vial were run after each 10 exosome samples. The sample was injected using a splitless mode with a volume of 1 μl. A DB-5 ms capillary column, which was 30 m long and 250 μm in diameter with a 0.25-μm film thickness consisting of 5% diphenyl cross-linked with 95% dimethylpolysiloxane, was used to separate the metabolites. Helium (99.9996%) was used with a constant flow rate of 1 ml/min. The GC oven temperature was initially set to 80 ℃ and held for 2 min. The temperature was gradually increased from the initial temperature to 180 ℃ at a rate of 10 ℃ per minute. It was then further increased to 230 ℃ at a rate of 6 ℃ per minute and finally to 295 ℃ at a rate of 40 ℃ per minute. The temperature was maintained at a constant level at 295 ℃ for 8 min. The temperatures for the injection, transfer interface, and ion source were set to 270 ℃, 260 ℃, and 220 ℃, respectively. The mass range was set from 30 to 600 with electron impact ionization of 70 eV. The acquisition rate was 20 spectra per second. The obtained files from the GC–TOFMS analysis were exported in NetCDF format by using ChromaTOF software. (v4.44, Leco Co., Los Angeles, CA) [36]. The CDF files underwent several preprocessing steps, including baseline correction, denoising, smoothing, alignment, time-window splitting, and multivariate curve resolution. These steps were performed by using a toolkit developed by MATLAB 7.0 (The MathWorks Inc. Natick, MA), R 10.2 (Lucent Technologies), and JavaSE 1.6 (Sun Microsystems). Data quality control was ensured by using the internal standard and QC, whereas data normalization was performed by using QC. The ion peaks that were generated by the internal standard were removed to avoid any interference in the final results.

Identification of metabolic profiles

By using the GC–TOFMS analysis and by comparing mass fragments and recent times (RTs) with the National Institute of Standards and Technology (NIST) 05 and our laboratory libraries, we annotated 127 metabolites. Our libraries encompassed over 800 metabolites and are continuously expanding. A principal component analysis (PCA) score plot based on the samples from the aging group and the normal control group did not exhibit distinct clusters, thus indicating that they were not separated from each other. Partial least-squares-discrimination analysis (PLS-DA) and orthogonal partial least-squares-discrimination analysis (OPLS-DA) models were used to visualize the metabolic differences among the aging and normal control groups. The R2X, R2Y, and Q2Y values of the OPLS model were nearly 1.0 for the aging and normal control groups, thus indicating a good ability to explain and predict variations in the X and Y matrices. The resultant P values for all of the metabolites were subsequently adjusted to account for multiple tests by using a false discovery rate (FDR) method. Metabolites with both multivariate and univariate statistical significance (variable importance in projection, VIP > 1 and $P < 0.05$) were considered to be potential markers capable of differentiating PC from the controls. Additionally, the KEGG database was utilized to identify the affected metabolic pathways.

Data analysis and statistics

Statistical analysis for acquiring data was performed by using SPSS (SPSS, Chicago, IL) and SIMCA-P 12.0.1 + (Umetrics, Umea, Sweden). For the normally distributed continuous variables, Student's t test was used for comparisons between the different groups. Otherwise, the Mann−Whitney U test was used. The OPLS models were validated by using a permutation test. Qualitative data were compared by using either the Chi-square test or Fisher's exact test. Spearman's rank correlation analysis was performed to estimate the correlation between the detected metabolites and the clinical characteristics of all of the subjects, we performed. A statistically significant result was defined as $P < 0.05$.

Results
Characteristics of patients

The mean basal serum FSH (mIU/ml) was lower in the young age group than in the advanced age group. The

number of retrieved oocytes was significantly higher in the young age group than in the advanced age group. There was no significant difference between the two

Table 1 Characteristics of patients

Parameters	Young age group ($n=30$)	Advanced age group ($n=30$)	P
Age (years)	28.97 ± 0.53	44.13 ± 0.58	< 0.05
BMI (kg/m^2)	21.35 ± 0.37	22.38 ± 0.37	0.52
Basal serum FSH (mIU/ml)	6.80 ± 0.64	14.58 ± 2.65	< 0.05
Basal serum LH (mIU/ml)	5.65 ± 0.71	5.74 ± 0.89	0.94
Basal serum estradiol (pg/ml)	51.54 ± 6.68	37.53 ± 4.71	0.09
Number of oocytes retrieved	16.5 ± 1.64	3.33 ± 0.72	< 0.05

All of the results are presented as the mean ± SEM

BMI body mass index, *FSH* follicle-stimulating hormone, *LH* luteinizing hormone

groups in basal serum luteinizing hormone (LH, mIU/ml) or basal serum estradiol (pg/ml) (Table 1).

Isolation and characterization of exosomes derived from FF of young controls and advanced age

Exosomes derived from FF were characterized via Western blot, TEM, and NTA. The NTA and TEM findings were in conjunction with the previously documented traits of exosomes (Fig. 1A and Fig. 1C). The NTA and TEM results were consistent with previously reported characteristics of exosomes [17, 35, 37, 38]. Western blot results showed that three exosomal markers (CD63, TSG101, and HSP70) were detected in exosomes derived from FF (Fig. 1B). In addition, we found that exosome concentration (number of particles per ml FF) and exosomal protein concentration (µg exosomal protein/µl FF) from FF in the advanced age group were slightly lower than those from the young age group; however, the difference was not significant (Fig. 1D, E, all $P > 0.05$).
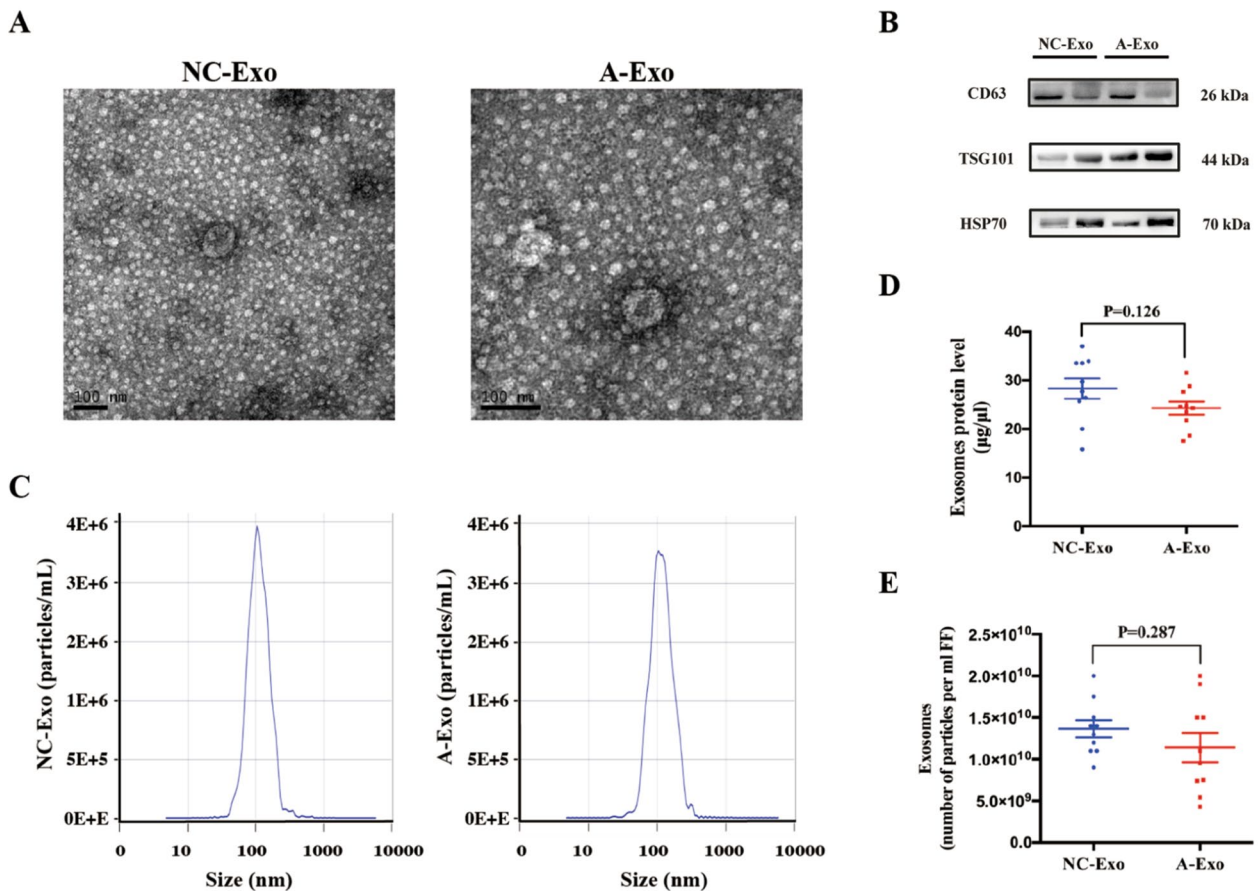

Fig. 1 Characterization of exosomes derived from the FF of patients in the advanced age group and young age group. **A** TEM images of isolated exosomes with a saucer-like shape limited by a lipid bilayer. **B** Western blot analysis of exosomal surface markers CD63, TSG101, and HSP70 in FF-derived exosomes of the young age group and advanced age group. **C** The size distribution of exosomes obtained from FF of the young age group and advanced age group was analysed by NTA. **D** Exosomal protein concentration (ug exosomal protein/µl FF) in the FF of the young age group and advanced age group. **E** Exosomes concentration (number of particles per ml FF) in the FF of the young age group and advanced age group

Main metabolite groups in FF exosomes

Multivariate analysis via principal component analysis (PCA) did not demonstrate a perfect separation between the analysed data groups for each group (PC1 variance: 26.83%; PC2 variance: 12.61%) (Fig. 2A). To further distinguish the differences in metabolic profiles between the two groups, we applied an advanced supervisory discriminant model known as OPLS-DA (Fig. 2B). A clear discrimination between the NC-Exo and A-Exo groups was apparent in the scatter plot of the OPLS-DA model
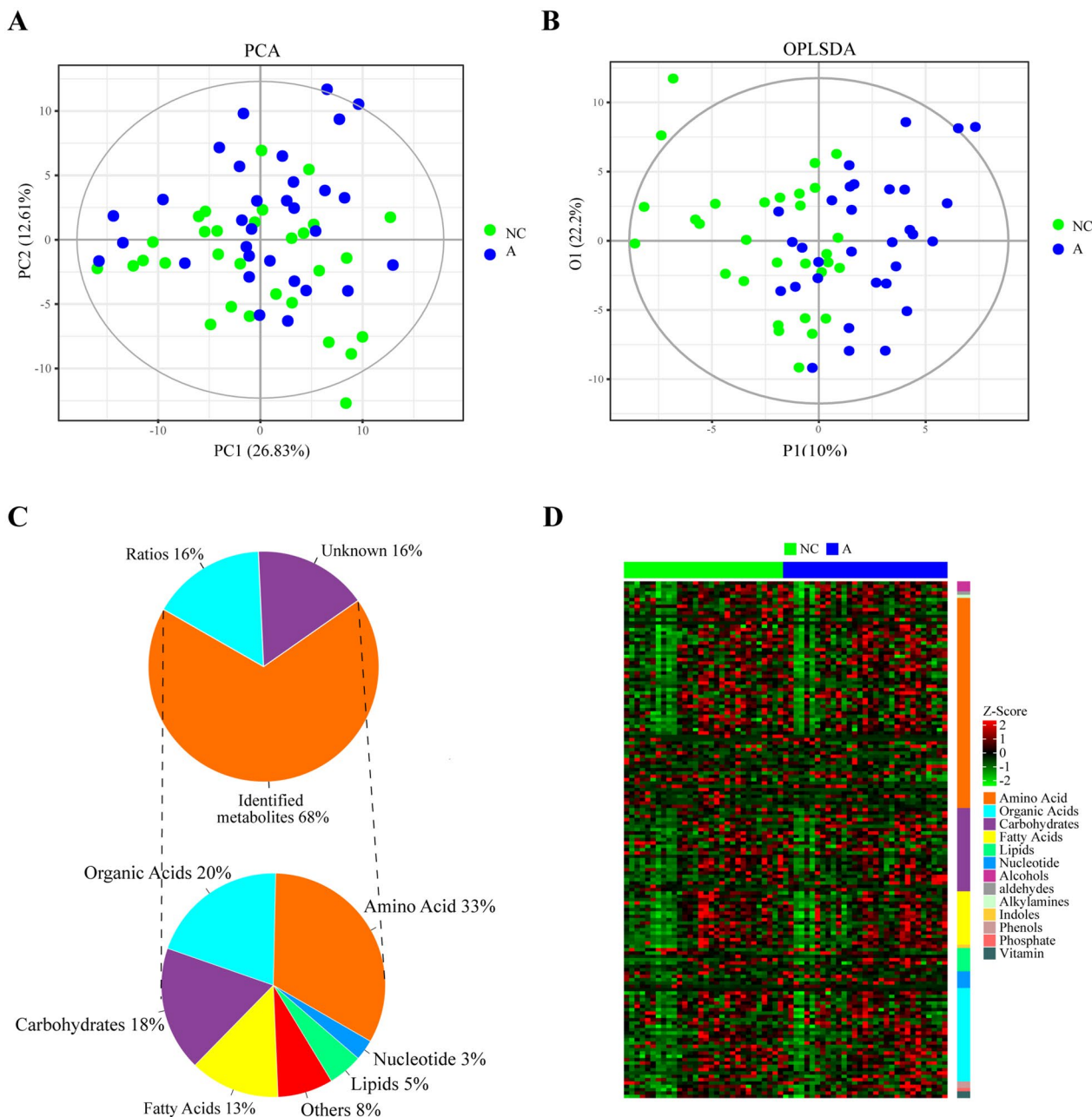

Fig. 2 Metabolomic analysis of exosomes derived from FF of the advanced age group and young group. **A** PCA scores of metabolite profiles between the advanced age group and young age group. **B** OPLS-DA model of metabolite profiles between the advanced age group and the young age group. **C** The proportion of identified and unknown metabolites and other components in the sample, as well as the categories and the proportion of identified metabolites in the sample, were also analysed separately. **D** Z score heatmap of an overview of metabolic profiles in all of the samples. The heatmap colour code indicates relative metabolite abundance: red indicates increased levels, and green indicates decreased levels in advanced age vs. young control

Gu *et al. European Journal of Medical Research*　　　(2024) 29:4

Page 6 of 12

(Fig. 2B). Of all of the samples, identified metabolites accounted for 68%, unknown metabolites accounted for 16%, and other components accounted for 16% (Fig. 2C). The identified metabolites mainly included amino acids (33%), carbohydrates (18%), organic acids (20%), fatty acids (13%), lipids (5%), and nucleotide (3%) (Fig. 2C). To further understand the alterations in metabolites in the two groups, we used a Z score heatmap to provide an overview of the metabolic profile in all of the samples, which showed the relative change in each metabolite across all of the samples (Fig. 2D).

Age-related changes in the FF exosomal metabolites

We detected 157 metabolites. Of these, 127 metabolites were identified by using *JiaLib*™ (one of the largest metabolomics libraries in the world) and 30 metabolites were not identified. Table 2 shows the differentially abundant metabolites that were obtained based on unidimensional statistical analysis in FF exosomes between patients in the young age group and advanced age group, including alcohols, alkylamines, amino acids, carbohydrates, fatty acids, indoles, nucleotides, and organic acids. In particular, we found that the levels of the 13 identified metabolites (one alcohol [2-hydroxypyridine], four amino acids [i.e. ratio of L-glutamic acid/L-glutamine, L-threonine, beta-alanine, and glutathione], two carbohydrates [alpha-lactose, D-maltose], one fatty acid [oleic acid], two nucleotides [inosine and cytidine] and three organic acids [the ratio of homogentisic acid/4-hydroxyphenylpyruvic acid, taurine and fumaric acid]) were significantly higher in the advanced age group than in the young age group, with fold changes ranging from 1.075 to 2.723 ($P \leq 0.05$). Moreover, four identified metabolites (three amino acids [the ratio of 4-hydroxyphenylpyruvic acid/L-tyrosine, the ratio of L-glutamine/L-glutamic acid and the ratio of ketoleucine/L-leucine], and one organic acid [malonic acid]) were lower in the advanced

Table 2 Differences in metabolite expression in FF exosomes between patients in the young age group and advanced age group

Class	Name	P	FC
Alcohols	2-Hydroxypyridine	2.00E−02	1.176
Alkylamines	Spermidine	0.072	1.14
Amino acid	Ratio of 4-hydroxyphenylpyruvic acid/L-tyrosine	1.70E−03	0.603
	Ratio of L-glutamine/L-glutamic acid	4.70E−03	0.562
	The ratio of L-glutamic acid/L-glutamine	4.70E−03	1.781
	Ratio of ketoleucine/L-leucine	2.00E−02	0.403
	L-Threonine	2.30E−02	1.326
	Beta-Alanine	2.90E−02	1.301
	Glutathione	3.80E−02	1.378
	L-Arginine	0.052	1.62
	L-Alloisoleucine	0.057	1.124
	Pyroglutamic acid	0.059	1.311
	Ketoleucine	0.082	0.772
	L-Phenylalanine	0.082	1.219
	Aminoadipic acid	0.096	0.72
Carbohydrates	Alpha-Lactose	5.20E−03	1.561
	D-Maltose	7.50E−03	1.833
	L-Arabitol	0.056	1.518
Fatty acid	Oleic acid	3.50E−02	2.668
	Dodecanoic acid	0.08	0.838
Indoles	Melatonin	0.057	1.283
Nucleotide	Inosine	1.30E−02	1.383
	Cytidine	2.90E−02	1.415
Organic acids	Ratio of homogentisic acid/4-Hydroxyphenylpyruvic acid	1.10E−02	2.723
	Taurine	3.60E−02	1.338
	Malonic acid	5.00E−02	0.694
	Fumaric acid	5.00E−02	1.075
	3-Hydroxyanthranilic acid	0.063	1.246
	4-Hydroxyphenylpyruvic acid	0.07	0.578

age group than in the young age group, with fold changes ranging from 0.403 to 0.694 ($P \leq 0.05$).

Analysis of enrichment pathways between the two groups

The enhanced volcano diagram shown in Fig. 3A shows the differentially abundant metabolites that were screened based on the one-dimensional criteria (*P* value and fold change value). In this figure, *P* values set thresholds of 0.05 and 0.1, and $\log_{1.2}$ FC (FC is a fold change, multiple of intergroup change) set thresholds of ± 1. As shown in the volcano map based on multidimensional statistics, the highlighted metabolites in the upper right corner were significantly increased in the sample of the advanced age group versus the young age group, whereas the highlighted metabolites in the upper left corner were

significantly decreased in the sample of the advanced age group versus the young age group (Fig. 3A). Figure 3B shows a Z score heatmap of significantly differentially abundant metabolites between the two groups. The results were consistent with the differentially abundant metabolite table (Table 2). The pathway analysis that was conducted on differentially abundant metabolites demonstrated significant KEGG pathway enrichment. Differentially expressed metabolites in the pathways were mainly related to pyrimidine metabolism, taurine and hypotaurine metabolism, and valine, leucine, and isoleucine biosynthesis (Fig. 3C).

Given the robust associations of some exosomal metabolites with aging, we, therefore, explored whether exosomal metabolites could serve as biomarkers to
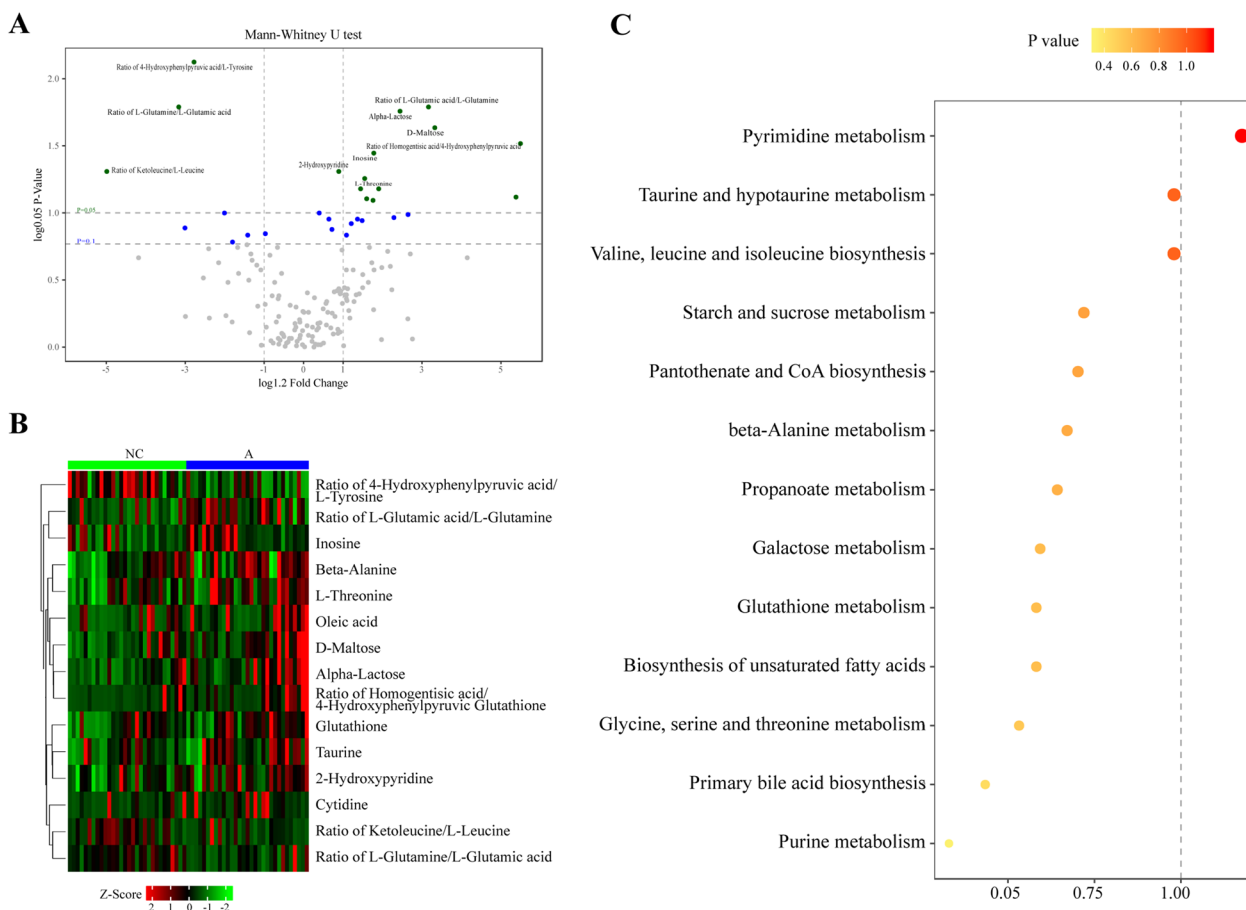

Fig. 3 Analysis of differentially abundant metabolites and enrichment pathways between the two groups. **A** Enhanced volcanic map of differentially abundant metabolites based on the one-dimensional criteria (*P* value and fold change value). Levels of each metabolite between the advanced age group and young age group were tested with the Mann–Whitney *U* test. In the volcano plot, the log 0.05 *P* value (y-axis) was plotted against the fold change (x-axis). The metabolites with $0.05 \leq P \leq 0.1$, $P < 0.05$, and $P \geq 0.1$ are shown with blue, green, and grey points, respectively. **B** Z score heatmap of an overview of differentially abundant metabolites in FF exosomes of the advanced age group and young age group. The heatmap displays the relative metabolite abundance, with red and green indicating increased and decreased levels in the advanced group versus the young group, respectively. **C** Metabolite set enrichment analysis depicted the metabolic pathways in which significant differentially expressed metabolites are involved between the advanced age group and young age group

differentiate between patients in the advanced age group and the young age group. A total of 29 metabolites were subjected to a random forest classifier for potential metabolite biomarker analyses, and a set of 15 metabolites (the ratio of ʟ-glutamine/ʟ-glutamic acid, the ratio of ʟ-glutamic acid/ ʟ-glutamine, inosine, the ratio of 4-hydroxyphenylpyruvic acid/ ʟ-tyrosine, glutathione, 2-hydroxypyridine, taurine, beta-alanine, the ratio of ketoleucine/ ʟ-leucine, the ratio of homogentisic acid/4-hydroxyphenylpyruvic acid, alpha-lactose, ᴅ-maltose, ʟ-threonine, cytidine, and oleic acid) were identified as the optimal set of metabolites to discriminate between the advanced age group and young age group (Fig. 4A). In the variable importance in projection (VIP) variable importance analysis, the differentially abundant metabolite importance between the young age group and the old group was projected (Fig. 4B). We used the 15 metabolites to draw a receiver operating characteristic (ROC) curve, and the area under the curve (AUC) was used as an estimate of the predictive accuracy of the panel of biomarkers. By using the top four important metabolites as indicated by the VIP model (Fig. 4B), an AUC higher than 0.70 was obtained (Fig. 4C). This favourable AUC value demonstrated that these metabolites have a high predictive ability to differentiate patients in the advanced age group from the those in young age group. This result corroborates with the previous models that were built (OPLS-DA), which all performed well in differentiating between the two groups with low error rates. These results suggested that the 15 FF exosomal metabolites may be biomarkers to differentiate between patients in the advanced age group and the young age group.

Correlation analysis between exosomal metabolites and clinical indicators

To analyse the correlation between the detected metabolites and the clinical characteristics of all of the subjects, we performed Spearman's rank correlation analysis. The overall analysis displayed a clear separation between some clinical characteristics and the concentrations of the metabolites. Among the metabolites that are differentially expressed in FF, some are related to oocyte count and hormone levels (Fig. 5). Several metabolites (i.e. taurine, lactose, glutathione, maltose, oleic acid, melatonin, oxoglutaric acid, 2-hydroxypyridine, citrulline, arabinose, ʟ-arabitol, and pyroglutamic acid) increased with age, and other metabolites (i.e. amino adipic acid, alpha-ketoisovaleric acid, uric acid, hydroxyphenyl pyruvic acid, keto leucine, malonic acid, and glutamine) decreased with age. These results demonstrated an age-related trend in metabolites.

Discussion

In this study, we observed the metabolic changes in of exosomes in the FF of women of advanced age (which is a natural process) rather than women with premature ovarian failure (POF) or diminished ovarian reserve (DOR). We identified 17 differentially expressed metabolites in the exosomes from FF of young age and women of advanced age ($P \leq 0.05$, FC > 1 or FC < 1), which were significantly related to the regulation of oocyte number and hormone levels.

Previous studies have reported on the characteristics of FF metabolites rather than exosomes [39]; additionally, other studies have identified the metabolic profile of FF and attempted to find potential biomarkers of oocyte developmental competence [40–43]. Targeted metabolomics has demonstrated a significant reduction in polyunsaturated choline plasmalogens and a lower dimethylarginine/arginine ratio in the FF of patients with diminished ovarian reserve [44]. In addition, analyses of the FF metabolomics profile demonstrated decreased follicular glucose levels and increased lactate levels in advanced maternal-age women, which may suggest that follicular glycolysis is overactive [45, 46]. Unlike these studies, our study focused on metabolites in FF exosomes derived from females of advanced age. Exosomes have a unique composition of inclusions compared to the humoral environment, and the inclusions are more stable because of membrane encapsulation. In the present study, we found that exosome concentration and exosomal protein concentration from FF in the advanced age group were slightly lower than those from the young age group (Fig. 1D, E), which is consistent with a recent study showing that circulating exosome concentration decreases with aging [47]. Additionally, the circulating exosomes of older individuals were more easily internalized by B cells and had higher major histocompatibility complex II (MHC-II) expression on monocytes than exosomes from younger people, thus suggesting that the decreased concentration of exosomes with age may be partially attributed to increased internalization [47].

Our analysis of metabolites in the FF of exosomes showed increased oleic acid (FC = 2.668, $P < 0.05$), alpha-lactose (FC = 1.561, $P < 0.05$), and d-maltose (FC = 1.833, $P < 0.05$) levels in the advanced age group compared with the young age group, which may partly reflect age-related changes in ovarian glycolysis and fatty acid metabolism in older women. Follicles utilize a predominantly glycolytic method of adenosine triphosphate (ATP) production [48]. Oleic acid is a long-chain unsaturated omega-9 fatty acid and is a major monounsaturated fatty acid in the lipid extracts of bovine, sheep, pig [49, 50], and human oocytes [51]. Other studies have found that oleic acid had a positive effect on lipid storage, oocyte
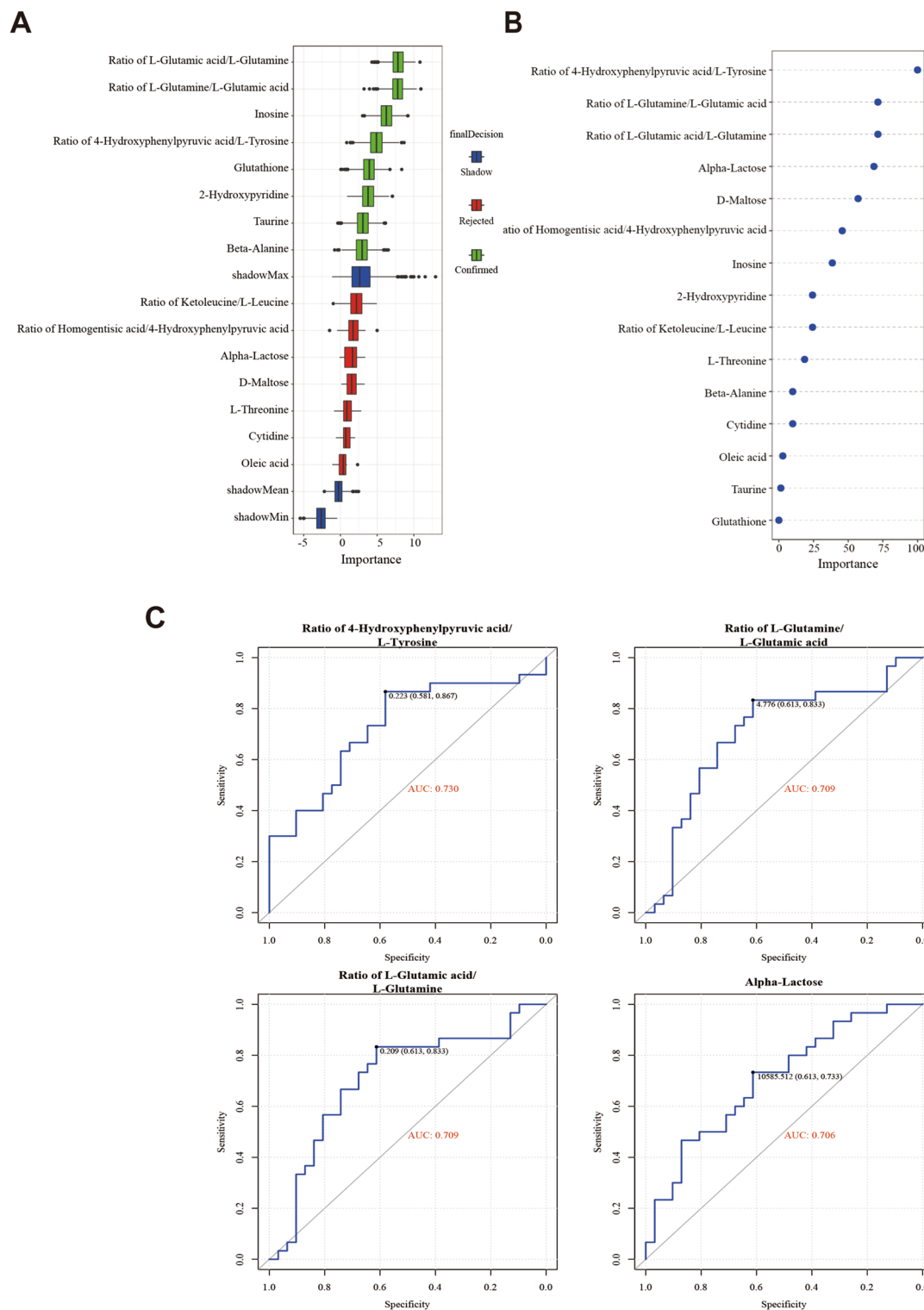
Fig. 4 Comparison of the importance of differentially abundant metabolites between the two groups. **A** Random forest assessment of differentially abundant metabolite importance between the two groups. **B** VIP analysis of differentially abundant metabolites between the young age group and advanced age group. **C** Differentially abundant metabolite ROC analysis. The ROC curve of the four metabolites with the largest AUC between the two groups
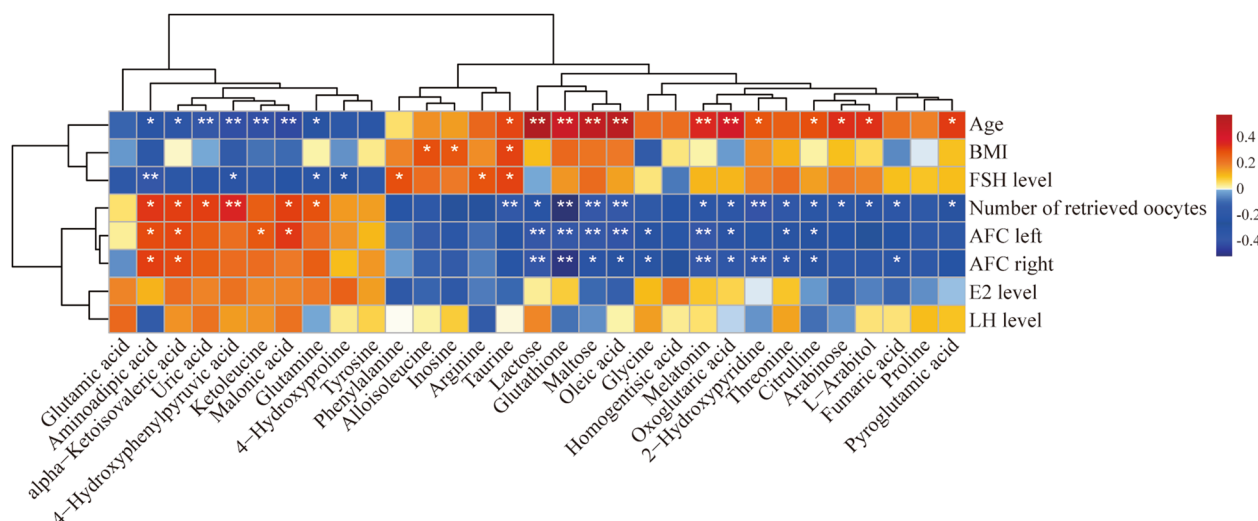
Fig. 5 Correlation analysis between exosomal metabolites and clinical indicators. The concentrations of the metabolites from the young age group and advanced age group were normalized according to protein tissue contents. The colours in the heatmap cells indicate correlation; red indicates positive, and blue indicates negative

maturation, and subsequent embryo development in the cows, thus overcoming the adverse effects of the other two main saturated fatty acids (palmitic and stearic acids) [52]. Several in vitro studies have also indicated that the increased oleic acid concentration in the FF of the advanced age group may reflect decreased lipid storage, insufficient energy storage, and lower cell metabolism.[53–55]. In addition, increased alpha-lactose and d-maltose in the concentration of FF exosomes from the advanced age group may reflect enhanced glycolysis, including increased glycogen decomposition and the conversion of lactose to glucose to provide energy for follicular development [56, 57].

In our results, significantly increased levels of glutathione (FC = 1.378, $P < 0.05$), beta-alanine (FC = 1.301, $P < 0.05$), and L-threonine (FC = 1.326, $P < 0.05$) were identified in the advanced age group. Glutathione exerts antioxidative and free radical-scavenging roles. The concentration of glutathione in oocytes can indicate the stage of oocyte maturation [58, 59]. Studies have found that glutathione levels decline with age [60]. Moreover, the generation of glutathione, which is reversible with antioxidants, is one of the most significant inadequacies of antioxidant defences in aging cells [61]. In our results, significantly increased glutathione in the concentration of exosomes of FF in the advanced age group may indicate increased antioxidant production. In normal metabolism, the ammonium produced by cells is eliminated by the synthesis of alanine, glutamic amide, and the urea cycle. The build-up

of ammonium in the FF can lead to metabolic perturbations, alterations in gene expression patterns, and a decline in embryo viability [61]. A likely role for the increased alanine and threonine level in the exosomes of FF in the advanced age group that were observed in this study may be represented by the removal of excess ammonium.

Furthermore, significantly increased levels of inosine (FC = 1.383, $P < 0.05$), cytidine (FC = 1.415, $P < 0.05$), and taurine (FC = 1.338, $P < 0.05$) were observed in the advanced age group. Cytidine plays an important role in phosphoinositide signalling and the synthesis of lipids [62]. In addition to being incorporated into nucleic acids, the circulating pyrimidine known as cytidine can act as a substrate for the salvage pathway of pyrimidine nucleotide synthesis and as a precursor of the cytidine triphosphate (CTP) that is needed in the biosynthesis of phosphatidylcholine and phosphatidylethanolamine [63]. The increased levels of inosine and cytidine in patients of advanced age may reflect the change in nucleotide stress expression and the synthesis of more transfer ribose nucleic acids (tRNAs) and lipids, which support the expression of stress response proteins and energy substrates. The effects of taurine on female reproduction may be primarily achieved by regulating the activities of hypothalamic–pituitary–ovarian axis-related hormones [64]. Increased taurine in the concentration of exosomes of FF in the advanced age group may indicate the compensatory enhancement of ovarian endocrine function with age.

Conclusions

In this study, we identified differences in the metabolites of exosomes from FF between women of young age and advanced age. These different metabolites have certain significance for revealing the mechanism of age-related changes in ovarian reproductive function. Additionally, these findings may lead to a better understanding of the nutritional profiles of the follicles with age.

Availability of data and materials
The data that were used in the study are available from the corresponding author upon reasonable request.

Declarations

Ethics approval and consent to participate
This study was approved by the Scientific and Ethical Committee of the Shanghai First Maternity and Infant Hospital affiliated with Tongji University. All of the participants gave their written informed consent and the collection of samples was approved.

Competing interests
All of the authors confirm that there are no conflicts of interest.

References

1. Broekmans FJ, et al. Female reproductive ageing: current knowledge and future trends. Trends Endocrinol Metab. 2007;18(2):58–65.
2. Crawford NM, Steiner AZ. Age-related infertility. Obstet Gynecol Clin North Am. 2015;42(1):15–25.
3. Kenny LC, et al. Advanced maternal age and adverse pregnancy outcome: evidence from a large contemporary cohort. PLoS ONE. 2013;8(2): e56583.
4. Tan TY, et al. Female ageing and reproductive outcome in assisted reproduction cycles. Singapore Med J. 2014;55(6):305–9.
5. Tatone C, et al. Cellular and molecular aspects of ovarian follicle ageing. Hum Reprod Update. 2008;14(2):131–42.
6. Eichenlaub-Ritter U, et al. Age related changes in mitochondrial function and new approaches to study redox regulation in mammalian oocytes in response to age or maturation conditions. Mitochondrion. 2011;11(5):783–96.
7. Fortune JE. Ovarian follicular growth and development in mammals. Biol Reprod. 1994;50(2):225–32.
8. Hailay T, et al. Extracellular vesicle-coupled miRNA profiles in follicular fluid of cows with divergent post-calving metabolic status. Sci Rep. 2019;9(1):12851.
9. Revelli A, et al. Follicular fluid content and oocyte quality: from single biochemical markers to metabolomics. Reprod Biol Endocrinol. 2009;7:40.
10. Hennet ML, Combelles CM. The antral follicle: a microenvironment for oocyte differentiation. Int J Dev Biol. 2012;56(10–12):819–31.
11. Shaaker M, et al. Fatty acid composition of human follicular fluid phospholipids and fertilization rate in assisted reproductive techniques. Iran Biomed J. 2012;16(3):162–8.
12. Hsieh M, Zamah AM, Conti M. Epidermal growth factor-like growth factors in the follicular fluid: role in oocyte development and maturation. Semin Reprod Med. 2009;27(1):52–61.
13. Edwards RG. Follicular fluid. J Reprod Fertil. 1974;37(1):189–219.
14. Raposo G, Stoorvogel W. Extracellular vesicles: exosomes, microvesicles, and friends. J Cell Biol. 2013;200(4):373–83.
15. Iraci N, et al. Focus on extracellular vesicles: physiological role and signalling properties of extracellular membrane vesicles. Int J Mol Sci. 2016;17(2):171.
16. Tkach M, Théry C. Communication by extracellular vesicles: where we are and where we need to go. Cell. 2016;164(6):1226–32.
17. Li H, et al. S100–A9 protein in exosomes derived from follicular fluid promotes inflammation via activation of NF-κB pathway in polycystic ovary syndrome. J Cell Mol Med. 2020;24(1):114–25.
18. Picca A, et al. Mitochondrial dysfunction and aging: insights from the analysis of extracellular vesicles. Int J Mol Sci. 2019;20(4):805.
19. Xu D, Tahara H. The role of exosomes and microRNAs in senescence and aging. Adv Drug Deliv Rev. 2013;65(3):368–75.
20. Robbins PD. Extracellular vesicles and aging. Stem Cell Investig. 2017;4:98.
21. Takasugi M. Emerging roles of extracellular vesicles in cellular senescence and aging. Aging Cell. 2018;17(2):e12734.
22. Palomo L, et al. Considerations for applying metabolomics to the analysis of extracellular vesicles. Front Immunol. 2014;5:651.
23. Simons M, Raposo G. Exosomes–vesicular carriers for intercellular communication. Curr Opin Cell Biol. 2009;21(4):575–81.
24. Royo F, et al. Differences in the metabolite composition and mechanical properties of extracellular vesicles secreted by hepatic cellular models. J Extracell Vesicles. 2019;8(1):1575678.
25. Iraci N, et al. Extracellular vesicles are independent metabolic units with asparaginase activity. Nat Chem Biol. 2017;13(9):951–5.
26. Hoffman JM, et al. Proteomics and metabolomics in ageing research: from biomarkers to systems biology. Essays Biochem. 2017;61(3):379–88.
27. da Silveira JC, et al. Cell-secreted vesicles in equine ovarian follicular fluid contain miRNAs and proteins: a possible new form of cell communication within the ovarian follicle. Biol Reprod. 2012;86(3):71.
28. Ng YH, et al. Endometrial exosomes/microvesicles in the uterine microenvironment: a new paradigm for embryo-endometrial cross talk at implantation. PLoS ONE. 2013;8(3): e58502.
29. Lopera-Vasquez R, et al. Effect of bovine oviductal extracellular vesicles on embryo development and quality in vitro. Reproduction. 2017;153(4):461–70.
30. Almiñana C, et al. Oviduct extracellular vesicles protein content and their role during oviduct-embryo cross-talk. Reproduction. 2017;154(3):153–68.
31. Sang Q, et al. Identification of microRNAs in human follicular fluid: characterization of microRNAs that govern steroidogenesis in vitro and are associated with polycystic ovary syndrome in vivo. J Clin Endocrinol Metab. 2013;98(7):3068–79.
32. Machtinger R, Laurent LC, Baccarelli AA. Extracellular vesicles: roles in gamete maturation, fertilization and embryo implantation. Hum Reprod Update. 2016;22(2):182–93.
33. Chang X, et al. Exosomes from women with preeclampsia induced vascular dysfunction by delivering sFlt (soluble fms-like tyrosine kinase)-1 and sEng (soluble endoglin) to endothelial cells. Hypertension. 2018;72(6):1381–90.
34. Jia L, et al. Maternal and umbilical cord serum-derived exosomes enhance endothelial cell proliferation and migration. Faseb j. 2018;32(8):4534–43.
35. Huang X, et al. Depletion of exosomal circLDLR in follicle fluid derepresses miR-1294 function and inhibits estradiol production via CYP19A1 in polycystic ovary syndrome. Aging (Albany NY). 2020;12(15):15414–35.
36. Guo Y, et al. Preoperative serum metabolites are associated with postoperative delirium in elderly hip-fracture patients. J Gerontol A Biol Sci Med Sci. 2017;72(12):1689–96.
37. Sohel MM, et al. Exosomal and non-exosomal transport of extra-cellular microRNAs in follicular fluid: implications for bovine oocyte developmental competence. PLoS ONE. 2013;8(11): e78505.

38. Hung WT, et al. Extracellular vesicles from bovine follicular fluid support cumulus expansion. biol Reprod. 2015;93(5):117.

39. Yang J, et al. Human follicular fluid shows diverse metabolic profiles at different follicle developmental stages. Reprod Biol Endocrinol. 2020;18(1):74.

40. Piñero-Sagredo E, et al. NMR metabolic profile of human follicular fluid. NMR Biomed. 2010;23(5):485–95.

41. Wallace M, et al. An investigation into the relationship between the metabolic profile of follicular fluid, oocyte developmental potential, and implantation outcome. Fertil Steril. 2012;97(5):1078-84 e1—8.

42. Xia L, et al. Metabolomic profiling of human follicular fluid from patients with repeated failure of in vitro fertilization using gas chromatography/mass spectrometry. Int J Clin Exp Pathol. 2014;7(10):7220–9.

43. O'Gorman A, et al. Metabolic profiling of human follicular fluid identifies potential biomarkers of oocyte developmental competence. Reproduction. 2013;146(4):389–95.

44. de la Barca JMC, et al. Targeted metabolomics reveals reduced levels of polyunsaturated choline plasmalogens and a smaller dimethylarginine/arginine ratio in the follicular fluid of patients with a diminished ovarian reserve. Hum Reprod. 2017;32(11):2269–78.

45. Dogan B, et al. High-resolution (1)H-NMR spectroscopy indicates variations in metabolomics profile of follicular fluid from women with advanced maternal age. J Assist Reprod Genet. 2020;37(2):321–30.

46. Da Broi MG, et al. Influence of follicular fluid and cumulus cells on oocyte quality: clinical implications. J Assist Reprod Genet. 2018;35(5):735–51.

47. Eitan E, et al. Age-related changes in plasma extracellular vesicle characteristics and internalization by leukocytes. Sci Rep. 2017;7(1):1342.

48. Boland NI, et al. Characterization of follicular energy metabolism. Hum Reprod. 1994;9(4):604–9.

49. Dunning KR, Russell DL, Robker RL. Lipids and oocyte developmental competence: the role of fatty acids and β-oxidation. Reproduction. 2014;148(1):R15-27.

50. Prates EG, et al. Fatty acid composition of porcine cumulus oocyte complexes (COC) during maturation: effect of the lipid modulators trans-10, cis-12 conjugated linoleic acid (t10, c12 CLA) and forskolin. in Vitro Cell Dev Biol Anim. 2013;49(5):335–45.

51. Matorras R, et al. Fatty acid composition of fertilization-failed human oocytes. Hum Reprod. 1998;13(8):2227–30.

52. Aardema H, et al. Oleic acid prevents detrimental effects of saturated fatty acids on bovine oocyte developmental competence. Biol Reprod. 2011;85(1):62–9.

53. Coyral-Castel S, et al. Effects of unsaturated fatty acids on progesterone secretion and selected protein kinases in goat granulosa cells. Domest Anim Endocrinol. 2010;38(4):272–83.

54. Yenuganti VR, Viergutz T, Vanselow J. Oleic acid induces specific alterations in the morphology, gene expression and steroid hormone production of cultured bovine granulosa cells. Gen Comp Endocrinol. 2016;232:134–44.

55. Van Hoeck V, et al. Oocyte developmental failure in response to elevated nonesterified fatty acid concentrations: mechanistic insights. Reproduction. 2013;145(1):33–44.

56. Cetica P, et al. Activity of key enzymes involved in glucose and triglyceride catabolism during bovine oocyte maturation in vitro. Reproduction. 2002;124(5):675–81.

57. Chatterjee IB. Ascorbic acid metabolism. World Rev Nutr Diet. 1978;30:69–87.

58. Bai Y, et al. Follicular fluid metabolite changes in dairy cows with inactive ovary identified using untargeted metabolomics. Biomed Res Int. 2020;2020:9837543.

59. Grochowska R, et al. Genetic variation in stimulated GH release and in IGF-I of young dairy cattle and their associations with the leucine/valine polymorphism in the GH gene. J Anim Sci. 2001;79(2):470–6.

60. Huang Y, et al. Age-dependent metabolomic profile of the follicular fluids from women undergoing assisted reproductive technology treatment. Front Endocrinol. 2022;13: 818888.

61. Lane M, Gardner DK. Ammonium induces aberrant blastocyst differentiation, metabolism, pH regulation, gene expression and subsequently alters fetal development in the mouse. Biol Reprod. 2003;69(4):1109–17.

62. Berry G, et al. Phosphatidylinositol:myo-inositol exchange activity in intact nerve endings: substrate and cofactor dependence, nucleotide specificity, and effect on synaptosomal handling of myo-inositol. J Neurochem. 1986;46(4):1073–80.

63. Kennedy EP, Weiss SB. The function of cytidine coenzymes in the biosynthesis of phospholipids. J Biol Chem. 1956;222(1):193–214.

64. Mu T, et al. Effect of taurine on reproductive hormone secretion in female rats. Adv Exp Med Biol. 2015;803:449–56.

Publisher's Note